(28) Zeichner, G. R.; Schowalter, W. R. *J. Colloid Interface Sci.* **1979**, *71*, 237.
(29) Sato, T.; Sieglaff, C. L. *J. Appl. Polym. Sci.* **1980**, *25*, 1781.
(30) Nieuwenhuis, E. A.; Pathmamanoharan, C.; Vrij, A. *J. Colloid Interface Sci.* **1981**, *81*, 196.
(31) Vogelsberger, W. *J. Colloid Interface Sci.* **1982**, *88*, 17.
(32) van de Hulst, H. G. "Light Scattering by Small Particles"; Wiley: New York, 1957.
(33) Wallach, M. L.; Heller, W. *J. Chem. Phys.* **1961**, *34*, 1796.
(34) Kerker, M. "The Scattering of Light and Other Electromagnetic Radiation"; Academic Press: New York, 1969.
(35) (a) Sedláček, B.; Koňák, Č. *J. Colloid Interface Sci.* **1982**, *90*, 60 and literature cited therein. (b) Sedláček, B.; Zimmermann, K. *Polym. Bull.* **1982**, *7*, 531. (c) Sedláček, B.; Verner, B.; Bárta, M.; Zimmermann, K. *Collect. Czech. Chem. Commun.* **1979**, *44*, 2064. (d) Sedláček, B. *Ibid.* **1971**, *36*, 2625.
(36) Maron, S. H.; Pierce, P. E. *J. Polym. Sci., Part C* **1969**, *27*, 183.
(37) Huglin, M. B., Ed. "Light Scattering from Polymer Solutions"; Academic Press: London and New York, 1972.
(38) Elias, H.-G. "Macromolecules, Structure and Properties"; Wiley: New York, 1977; Vol. 1.
(39) Zollars, R. L. *J. Colloid Interface Sci.* **1980**, *74*, 163.
(40) Lifshitz, I. M.; Grosberg, A. Yu.; Khokhlov, A. R. *Rev. Mod. Phys.* **1978**, *50*, 683. (a) Lifshitz, I. M. *Zh. Eksp. Teor. Fiz.* **1968**, *55*, 2408.
(41) (a) Post, C. B.; Zimm, B. H. *Biopolymers* **1982**, *21*, 2123. (b) Post, C. B.; Zimm, B. H. *Ibid.* **1982**, *21*, 2139.
(42) (a) Flory, P. J.; Sundararajan, P. R.; DeBolt, L. C. *J. Am. Chem. Soc.* **1974**, *96*, 5015. (b) Sundararajan, P. R.; Flory, P. J. *Ibid.* **1974**, *96*, 5025.
(43) Belnikevitch, N. G.; Mrkvičková, L.; Quadrat, O. *Polymer* **1983**, *24*, 713.
(44) Wolff, C.; Silberberg, A.; Priel, Z.; Layec-Raphalen, M. N. *Polymer* **1979**, *20*, 281.
(45) Kuhn, W.; Majer, H. *Makromol. Chem.* **1956**, *18/19*, 239.

Structure of Poly(diacetylenes) in Solution†

Gerhard Wenz, Michael A. Müller, Manfred Schmidt, and Gerhard Wegner*

Institut für Makromolekulare Chemie, Universität Freiburg, D-7800 Freiburg i.Br., West Germany. *Received July 29, 1983*

ABSTRACT: The solution properties of poly(diacetylenes) [=(R)C—C≡C—C(R)]= were studied by using PTS-12 (R = $(CH_2)_4OSO_2C_6H_4CH_3$) and P3BCMU (R = $(CH_2)_3OCONHCH_2CO_2C_4H_9$) as the prime examples. The UV–vis, the resonance-Raman, and the ^{13}C-NMR spectra of the dissolved polymers may be interpreted by comparison with low molecular weight polyconjugated model substances as if the backbone skeleton consisted of segments of effective conjugation length n_{eff} decoupled from the other segments electronically by bond rotation. All three methods give the same value of n_{eff} of approximately 5–7 constitutive units. Light scattering and viscosity studies indicate, however, that the poly(diacetylenes) behave like a wormlike (Porod–Kratky) chain. The persistence length was determined for PTS-12 as 15–20 nm, corresponding to 30–40 constitutive units. In the framework of this model the backbone skeleton is continuously deformed down to the scale of the individual bonds. Thus, n_{eff} is recognized as being simply a number determined by using a calibration curve obtained from low molecular weight compounds, which are not necessarily models for the polymer. The blue-to-yellow transition observed to occur in solutions of P3BCMU was reinvestigated. In the yellow solutions P3BCMU exists molecularly dispersed in the form of a wormlike coil. The transition to the blue form, which is obtained by changing the temperature or solvent quality, was demonstrated to be an aggregation phenomenon and not a transition occurring within a single molecule (nonplanar-to-planar transition).

1. Introduction

Poly(diacetylenes) (PDA) (1) are unique among the synthetic organic polymers insofar as they can be obtained as perfect macroscopic single crystals by solid-state polymerization of suitably substituted diacetylenes (2).[1-7] The backbone of the PDA consists of conjugated double and triple bonds with the substituents R in all-trans-position with regard to the double bonds.

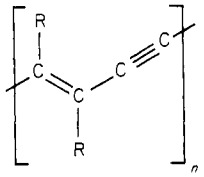

1

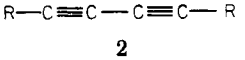

2

The conjugated backbone is the origin of the deep red to purple color and metallic luster of the polymer single crystals. The chain structure has been rigorously established by X-ray analyses in a large number of cases differing by the chemical nature of R[3,6-10] so that there does not remain any doubt that 1 gives the general and proper formulation of the bond sequence in PDAs. As expected, all the carbon atoms of the backbone are situated in a plane within the lattice and the chains are extended along a unique crystallographic axis, giving rise to an extremely anisotropic behavior of the PDA crystals concerning their mechanical, optical, and electrical properties. The field of PDA crystals, including the mechanism of solid-state polymerization,[11-14] has found widespread interest in recent years, and a number of reviews are available.[3,6,7,15] Very little is known, however, about the solution properties of PDA, owing to the extreme insolubility of most of the better investigated crystalline representatives of this class of polymers. Viscosity measurements and data on the solution spectra of some PDAs have been mentioned in the early reports on the solid-state polymerization of diacetylenes.[1,2,16] Since Patel et al. detected in 1978 that poly[4,6-decadiyne-1,10-diol bis((*n*-butoxycarbonyl)-methyl)urethane] (P3BCMU) (3) is a readily soluble polymer, the study of the solution properties of PDA chains[17-19] has attracted increasing interest. More recently, a fair number of soluble PDAs have been synthesized in our laboratory[20,21] and independently by Schulz and coworkers.[22,23] Some of the prominent representatives are mentioned in Table I. The most remarkable feature of these compounds is the dramatic blue shift of the optical absorption which is observed when the polymer crystals are dissolved. Typically, the crystals exhibit absorption spectra with a maximum around 600 nm, which shifts to approximately 450 nm on dissolution. Reprecipitation with concurrent recrystallization does not reconstitute the or-

† Dedicated to Professor Walter H. Stockmayer on the occasion of his 70th birthday with the warmest personal wishes.

0024-9297/84/2217-0837$01.50/0

Table I
Some Examples of Soluble Poly(diacetylenes) of General Structure

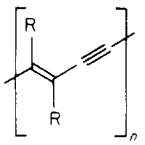

no.	R	typical solvents	abbreviation	ref
3	$(CH_2)_3OCONHCH_2CO_2$-*n*-C_4H_9	$CHCl_3$, DMF	P3BCMU	17-19, this work
4	$(CH_2)_4OSO_2C_6H_4CH_3$	CH_2Cl_2, DMF	PTS-12	20, this work
5	$CH_2OCONHC_6H_5$	HMPT-LiCl	HDU	1, 16, 42
6[a]	$CH_2OSO_2C_6H_4CH_3$	nitrobenzene	PTS-6	2, 16
7	$(CH_2)_9OCOCH(CH_3)_2$	$CHCl_3$		22, 23
8	$(CH_2)_9OCOCH_2C_6H_5$	$CHCl_3$		22, 23
9	$(CH_2)_9OCOCH_2$(1-naphthyl)	$CHCl_3$		22, 23
10	$(CH_2)_{11}CH_3$	decalin		24

[a] Only low molecular weight fractions are soluble.

iginal spectrum but rather produces a spectrum with at least two peaks, one somewhat red shifted from the solution peak and the other somewhat blue shifted from the original crystal spectrum. This effect has been treated by Chance and co-workers[18,25] and others[17,19] invoking the concept of effective conjugation length. A dissolved PDA chain is thought to consist of planar segments of the backbone extending over several π-bonds which are electronically decoupled from the adjacent segments through bond rotations. A distribution in segment lengths was invoked in order to treat the observed increase in half-width of the absorption peak of the dissolved vs. the single-crystal sample.

On the other hand, a random flight chain consisting of statistical elements of these segments of effective conjugation length cannot be easily reconciled with the expected restriction of bond rotation due to the polyconjugated chain structure. One would rater expect a wormlike chain, but then, the concept of a distribution of effective conjugation lengths is questionable, at least if understood as a static model.

Patel and Walsh,[19] who reported the first light scattering data on solutions of P3BCMU, evaluated their findings in terms of a rodlike structure of the dissolved macromolecules, and they also described an interesting type of phase transition occurring in such solutions. The deep yellow to orange color of the solution of P3BCMU in a good solvent shifts to deep blue on addition of a poor solvent or on cooling to low temperatures. They treated this effect as an intramolecular feature such that the initially rodlike molecule of short segments of effective conjugation length (i.e., the yellow state) transforms into an infinitely extended and fully conjugated rodlike molecule (i.e., the blue state).

In a recent short communication[20] we have already shown, that PDA most probably exist as coils in the form of their yellow solution and that the data of Patel and Walsh can be interpreted in the same way if one takes the chain length distribution and its effect on the light scattering properly into account.

The existing information on the solution properties of PDAs as related to their solid-state behavior seems, therefore, to indicate that there exist some rather interesting problems which will be encountered in all polymers with a polyconjugated backbone. The simplest representative of this class is, of course, poly(acetylene), for which a solvent has not been found so far[26] but for which the determination of effective conjugation length in the semicrystalline state by spectroscopic methods is an important current issue and bears relevance to the interpretation of the origin and the behavior of the charge transport in the conducting phase of this material.[27-29]

In the following we want to investigate whether the concept of the wormlike chain is applicable to the behavior of dissolved PDA chains and we want to discuss if there exists a relation between the so-called effective conjugation length and the shape as well as the behavior of the total macromolecule in solution. The polymer of the *p*-toluenesulfonate of dodeca-5,7-diyne-1,12-diol (PTS-12) (4) as well as P3BCMU (1) will be used as the actual examples.

2. Experimental Section

(a) Syntheses. The monomers corresponding to the polymers PTS-12 and P3BCMU were synthesized as described in the literature.[20,30] The polymers were obtained by solid-state polymerization of single crystals of the monomers induced by ^{60}Co γ-radiation at 30 ± 5 °C. A total dose of 3 Mrd (7 Mrd) was necessary to obtain a sample of 59% (90%) conversion to polymer in the case of PTS-12. The conversion was determined by measuring the OD of a solution of the partially converted sample as previously described.[20]

In the case of P3BCMU a total dose of 3 Mrd gave a yield of 36% polymer. Unreacted monomer was extracted by exhaustive washing of the sample by acetone.

(b) Physical Measurements. UV–vis spectra were obtained with a Perkin-Elmer Hitachi spectrophotometer. The solution spectra were run in a 1-cm cuvette in optical-grade solvents (band-pass 2 nm). Raman spectra were obtained with a Bruker laser Raman spectrometer RT 20 with the exciting laser line at 648 nm. ^{13}C-NMR solution spectra were run on a Bruker WH-90 (22.63 MHz) spectrometer; the concentration of the polymer was 100 mg mL^{-1}. The ^{13}C-NMR solid-state MAS spectra were obtained with a Bruker CXP-100 spectrometer (22.63 MHz).

Viscosity measurements were performed with an Ostwald viscosimeter. The influence of the shear gradient on the intrinsic viscosity was neglected.

The refractive index increments were determined on the refractometer of Brice Phoenix Precision Instruments calibrated by aqueous sodium chloride solutions using a concentration series of the polymers from 4.5 to 30 g L^{-1} in the solvents used for the light scattering experiments.

Light Scattering Measurements. Integrated light scattering (ILS) was performed at λ 546 and 578 nm by a Sofica light scattering photometer using a Hg high-pressure lamp (500 W) and interference filters for the selection of the wavelength.

ILS and quasi-elastic light scattering (QLS) were performed simultaneously at λ 647.1 nm with a Malvern K7023 96-channel correlator in connection with a self-designed light scattering spectrometer allowing simultaneous recording of the scattering intensity and of the time correlation function (TCF).[31] A krypton ion laser (Spectra Physics, Model 164-11) was used as the light source operating at 647.1-nm wavelength.

(c) Data Analysis of ILS and QLS. Due to the strong absorption of the polymers in their "yellow" solution (compare Figures 1 and 2) the measured intensity in the ILS experiment

Table II
Data Relevant for the Evaluation of the Light Scattering Intensities

	PTS-12			P3BCMU
	λ 546 nm	λ 578 nm	λ 633 nm	λ 647 nm
solvent	1,2-dichloroethane	1,2-dichloroethane	chloroform	chloroform
$\epsilon'/(cm^2\ g^{-1})$	120	10	0	0
$(dn/dc)/(cm^3\ g^{-1})$	0.267	0.220	0.190	0.141
n	1.4453	1.4453	1.4428	1.4428

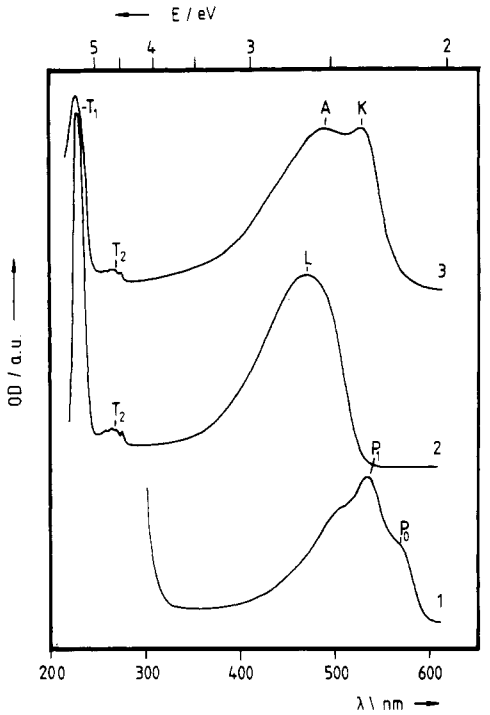

Figure 1. Comparison of the UV–vis spectra of PTS-12 in various states of aggregation: (1) partially polymerized single crystal of thickness $d = 0.1$ mm at 5% conversion; (2) solution of the polymer in 1,2-dichloroethane at a concentration $c = 3 \times 10^{-5}$ g cm^{-3}; (3) recrystallized film of thickness $d < 10$ μm. The individual spectra are displaced along the ordinate (optical density in arbitrary units) in order to avoid overlap.

had to be corrected for absorption effects.

With a cylindrical cuvette of diameter $2r$ the intensity of the primary beam I_0 will be reduced to I_M at the center of the cuvette according to

$$I_M = I_0 \times 10^{-\epsilon' cr} \tag{1}$$

Accordingly, the intensity of the scattered light will be reduced from i_M to i on its way from the center to the wall of the cuvette according to the equation

$$i = i_M \times 10^{-\epsilon' cr} \tag{2}$$

where ϵ' is the extinction coefficient of the polymer with weight concentration c. The ratio i_M/I_M is proportional to the scattering power of an isolated macromolecule thought to exist at the center of the cuvette. The ratio i/I_0 is, therefore, replaced by i_M/I_M and by comparison with a standard (benzene), the Rayleigh ratio R_θ was obtained

$$R_\theta = \frac{R_B}{i_B} i \times 10^{\epsilon' c 2r} \tag{3}$$

where the index B relates to the data of the standard. A Zimm diagram was then constructed, making use of the relations

$$\frac{Kc}{R_\theta} = \frac{1}{M_w} + \frac{\langle S^2\rangle_z}{3M_w} h^2 + 2A_2 c \tag{4}$$

with

$$K = \frac{4\pi^2 v_0}{N_A \lambda_0^4}\left(n \frac{dn}{dc}\right)^2; \qquad v_0 = 1\ \text{cm}^3 \tag{5}$$

$$h = (4\pi n/\lambda_0) \sin(\theta/2) \tag{6}$$

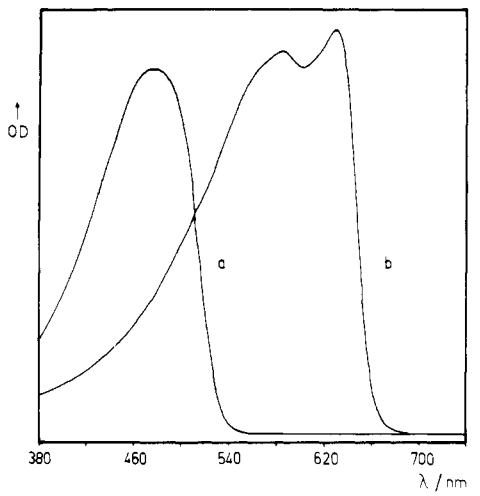

Figure 2. UV–vis spectra of solutions of P3BCMU: (a) "yellow" solution in chloroform, (b) "blue" solution obtained after addition of n-hexane (6/4 $CHCl_3$/hexane).

Here, M_w is the weight-average molecular weight, $\langle S^2\rangle_z^{1/2}$ is the root-mean-square radius of gyration, h is the scattering vector, A_2 is the second virial coefficient of the osmotic pressure, n is the refractive index of the solvent, dn/dc is the refractive index increment, θ is the scattering angle, and λ is the wavelength in vacuo. The data necessary to calculate the contrast factor K are given in Table II.

In the QLS experiment the time correlation function was analyzed according to the method of cumulants:

$$\ln g_1(t) = -\Gamma t + \tfrac{1}{2}\mu_2(\Gamma t)^2 - \tfrac{1}{6}\mu_3(\Gamma t)^3 \tag{7}$$

with $\Gamma \equiv -[d(\ln g_1(t))/dt]_{t\to 0}$. Γ is called the first cumulant, and $\mu_2 \equiv \Gamma_2/\Gamma^2$ and $\mu_3 \equiv \Gamma_3/\Gamma^3$ are describing the deviation from a single-exponential decay. Extrapolated to zero angle, the reduced first cumulant Γ/h^2 yields the z-average translational diffusion coefficient, $\lim_{h\to 0}(\Gamma/h^2) = D_z$. In all cases a second-order fit with respect to t described the time correlation function satisfactorily, and the third-order fit did not improve the variance significantly. For all samples the sample time τ was selected to fulfill the condition $\Gamma t_{max} = \Gamma \tau n_{max} \geq 5$, with n_{max} the last time channel in the correlator. Although our correlator is equipped with 96 time channels only, for the present measurements n_{max} equals 348, because a delay of 256τ occurs after the first 80 channels from 336τ to 348τ are used to monitor the base line. The slope of D_z against c for $h \to 0$ describes the concentration dependence of the translational diffusion coefficient according to

$$D_z(c) = D_z(0)(1 + k_d c) \tag{8}$$

3. Spectroscopic Investigations and Determination of the Effective Conjugation Length

(a) UV–vis Spectra. Experimental Results. Solutions of PDA are usually bright orange to yellow as compared to the deep red to purple color of the same materials in the single-crystal state. This is demonstrated for the case of PTS-12 (4, Table I) by Figure 1. Here, curve 1 is the absorption spectrum of a thin slice of a partially converted single crystal of the monomer. Due to the large extinction coefficient of the polymer it is practically impossible to obtain the absorption spectra of the pure

Table III
Solvatochromism of PTS-12

solvent	dielectric constant (20 °C) of solvent	refractive index n^{20}_D	absorp max of PTS-12 λ_{max}/nm	E/eV
$CHCl_3$	4.806	1.4459	462	2.68
CH_2ClCH_2Cl	10.65	1.4448	466	2.66
DMF	37.65	1.4305	474	2.62
nitrobenzene	35.74	1.5562	482	2.57

polymer single crystals directly. It has, however, been amply demonstrated that partially converted single crystals of the monomer can be understood as solid solutions of extended-chain macromolecules in the lattice of the yet unreacted monomer.[3,5,6,9,10] The two bands marked by P_1 and P_0 refer to two different modifications of the polymer PTS-12 which differ slightly with regard to their packing in the unit cell.[32,33] The monomer PTS-12 is known to undergo a phase transition during polymerization, which does not, however, disrupt the single-crystal texture. The peak P_0 (λ_{max} 570 nm) refers to the polymer formed within the initial monomer structure, and P_1 (λ_{max} 535 nm) is the band of the final polymer; in other words, the band P_0 disappears at higher conversions.[32]

The spectrum of the polymer dissolved in dichloroethane is shown by curve 2, where the peak maximum due to the backbone absorption is marked by L, and T_1 and T_2 refer to peaks caused by the side groups.

The extinction coefficient at λ 470 nm was found to be ϵ_{470} 16.7 × 10^3 L mol^{-1} cm^{-1}, referring to moles of constitutive units of the polymer in solution. The oscillator strength f was derived by integrating over the absorption peak between $\tilde{\nu}_1$ = 17 800 cm^{-1} and $\tilde{\nu}_2$ = 33 300 cm^{-1} according to the relation

$$f = 4.31 \times 10^{-9} \int_{\tilde{\nu}_1}^{\tilde{\nu}_2} \epsilon \, d\tilde{\nu} = 0.425 \qquad (9)$$

A solvatochromism is observed when different solvents are used. The peak maximum of the polymer absorption shifts to slightly lower energies if the polarity of the solvent is increased as indicated in Table III.

Films of the polymer may be cast from the solution. They are semicrystalline in nature and exhibit spectra like the one shown by curve 3, Figure 1. The peak labeled A resembles that in the solution spectrum although red shifted, and the one labeled K corresponds to the crystalline polymer (P_1 in curve 1) although somewhat blue shifted. The relative intensity of the two peaks depends on the preparation conditions, i.e., on the degree of crystallinity. One is, therefore, tempted to ascribe peak A (λ_{max} 490 nm) to the chain segments in the amorphous phase and peak K (λ_{max} 530 nm) to the ones in the crystalline phase.

The solution spectrum of P3BCMU (**3**, Table I) in the "yellow" and the "blue" state is shown in Figure 2. P3BCMU dissolves readily in chloroform and gives rise to a spectrum similar to the one of PTS-12. If, however, n-hexane is added to this yellow solution, a remarkable color change is observed, as demonstrated by spectrum b in Figure 2. This effect was first described by Patel et al.[17-19] and will be discussed later on.

(b) Absorption Maximum and Conjugation Length. Baughman and Chance[25,35,36] have suggested the treatment of the chain length dependence of the optical absorption of PDA in the same way as it is commonly accepted for oligoenes, since from the view point of overlapping π-orbitals the poly(diacetylene) backbone is analogous to that of the polyenes. Following the theory of Kuhn,[37] the optical bandgap E depends reciprocally on the number N of conjugated double bonds per molecule according to

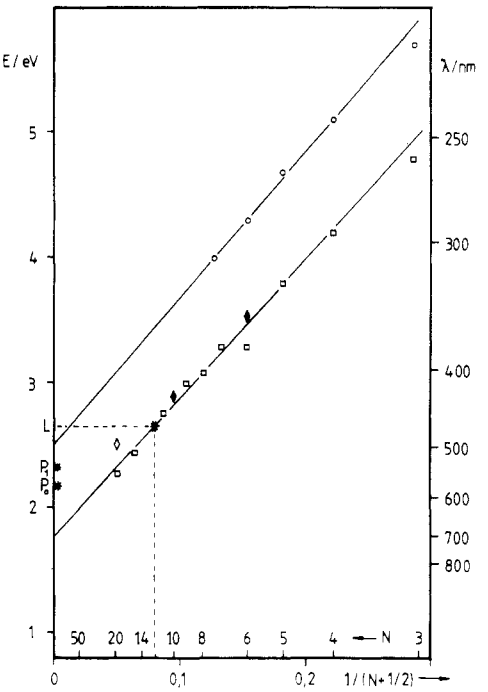

Figure 3. Plot of the energy of the optical transition of various polyconjugated compounds vs. the number of multiple bonds N: (○) polyynes t-Bu-$(C{\equiv}C)_N$-t-Bu;[38] (□) *trans*-polyenes CH_3-$(CH{=}CH)_N$$CH_3$[39] and carotinoids R-CH=CH-CH=C-$(CH_3)_{N/2}$-R;[40] (♦) polyenynes[41] t-Bu-$(C{\equiv}C)_2(CH{=}CH)_2(C{\equiv}C)_2$-$t$-Bu (**11**) and t-Bu-$[(C{\equiv}C)_2(CH{=}CH)_2]_2$-$(C{\equiv}C)_2$-$t$-Bu (**12**); (◇) oligomeric PTS-6 (**6**).[42] P_1 and P_0 relate to the peaks seen in the single-crystal spectrum in Figure 1, curve 1. L is the energy corresponding to the absorption peak marked L in Figure 1, curve 2.

$$E = V_0 + \left(\frac{h^2}{4mL_0^2} - \frac{V_0}{4} \right) \frac{1}{N + 0.5} \qquad (10)$$

V_0 is a parameter which may be understood as the amplitude of a sinusoidal potential which corrects the free electron gas model for bond length alternation. h is Planck's constant, m is the mass of the electron, and L_0 is the length of the unit of conjugation (one multiple plus one single bond in the case treated here).

Figure 3 shows a graph in which the energy of the optical transition of a fair number of oligoenes, oligoynes, and oligoenynes are plotted according to eq 10. Oligoenes and oligoynes are found to be situated on different straight lines; the value of V_0 for polyenes (1.75 eV) is lower than that for polyynes (2.5 eV). The only representatives of low molecular weight compounds with an enyne structure are compounds **11** and **12**. The energy of the optical excitation of these compounds is slightly larger than those of oligoenes of corresponding length.

Solutions of the oligomeric PTS-6 (**6**, Table I) show their absorption peak at E = 2.5–2.6 eV.[42] The average chain length of these soluble oligomers is between 7 and 15 units[9] and they fit reasonably well to the line of the oligoenes.

The oscillator strength per multiple bond in PTS-12 is f' 0.42/2 = 0.21. This value is much closer to the value reported for polyenes (f' = 0.25)[43] then to the value of polyynes (f' = 0.70),[38] giving another argument to believe that PDAs behave in much the same way as polyenes.

The effective conjugation length of a PDA may now be defined as the number of multiple bonds N which correspond to a certain excitation energy using the relationship for oligoenes in Figure 3 as the calibration curve.[35] Since

Table IV
^{13}C-NMR Chemical Shifts of PTS-12 and of the Corresponding Monomer in Solution and in the Solid State

polymer

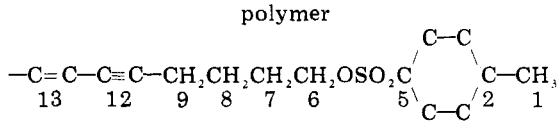

	monomer		carbon atom										
	—C≡	≡C—C≡	13	12	9	8	7	6	5	4	3	2	1
PTS-12, monomer solution	76.6	66.0	*a*	*a*	18.5	24.1	27.8	69.8	144.9	129.9	127.9	133.2	21.6
PTS-12, solution	*a*	*a*	129	99.4	34.7	24.7	28.1	70.6	144.4	129.7	128.1	133.2	21.8
PTS-12, single crystals as polymerized	*b*	63	*b*	106	36	28	31	72	149	132	128	137	20
PTS-12,[c] single crystals as polymerized	*a*	*a*	131	108	35.5	27	31	71	*a*	*a*	*a*	*a*	*a*
PTS-12, recrystallized	*a*	*a*	*a*	100	36	27	30	71	144	129	129	133	21

[a] Signal not present. [b] Signal hidden by other signals. [c] PTS-12-d_{14} (13).

the solution of PTS-12 was found to exhibit a maximum absorption at E = 2.66 eV, an effective conjugation length of N = 12 multiple bonds or $n_{eff} = N/2 = 6$ constitutive units is derived. A similar value has been found by Patel et al.[18] for the yellow solution of P3BCMU, in agreement with the spectra shown in Figure 2. It thus seems to be rather independent of the chemical structure of the substituents. Note that this determination of an effective conjugation length is purely heuristic since the excitation of a polyconjugated macromolecule is being compared to the one of a finite small molecule.

The difficulties and limitations in the interpretation of the meaning of effective conjugation lengths become also clear looking to the spectra of the crystalline PTS-12 reported in Figure 1. With the calibration curve of Figure 3, an n_{eff} = 13 for the peak labeled P_0 and n_{eff} = 10 for the one labeled P_1 are obtained, in gross disagreement with the extended-chain nature of the molecules in the partially polymerized but otherwise perfect crystal and the well-known average degree of polymerization P_n = 60 (P_1) and P_n = 500 (P_0) in the initial and in the final stage of conversion of PTS-12.[20,32]

(c) Raman Spectra. The Raman spectra of solid PDA have been investigated by a number of authors, both from an experimental and from a theoretical point of view.[7,44] Comparatively little work has been carried out on solutions of PDA, studies on P3BCMU being an exception.[25,45] Figure 4 shows the Raman spectrum of a solution of PTS-12 obtained with the exciting laser line at 648 nm, i.e., in the preresonance mode of excitation in order to avoid problems with the rather intensive fluorescence encountered if the exciting wavelength is chosen to be within the polymer absorption peak. The resonance-enhanced peaks marked 1 (ν = 2125 cm^{-1}) and 2 (ν = 1525 cm^{-1}) are assigned to the triple- and double-bond vibrations, respectively. The other peaks 3–6 are combination vibrations involving the side groups as well.

The frequency of a double-bond vibration of a conjugated system is thought to depend on the length of the system for similar reasons as does the energy of the optical transition.[44,46] For polyenes a plot of the frequencies of the double-bond vibration $\nu(N)$ vs. $(N + 1)^{-1}$ gives a straight line according to[27,45]

$$\nu(N) = 1459 + 720/(N + 1) = 1459 + 360/(n_{eff} + 0.5) \quad (11)$$

This empirical correlation allows for a determination of the effective conjugation length by comparison with the measured frequency of the double-bond vibration of the dissolved polymer, assuming that the same correlation is valid for polyenes (poly(acetylene)) and PDA. The value observed here (Figure 4) for PTS-12 corresponds to an n_{eff} of 5 constitutive units. Shand et al.[45] have found the same value of ν_2 = 1525 cm^{-1} for yellow solutions of P3BCMU, and these authors correlate this value to an n_{eff} = 7 using a correlation similar to the one given by eq 11.

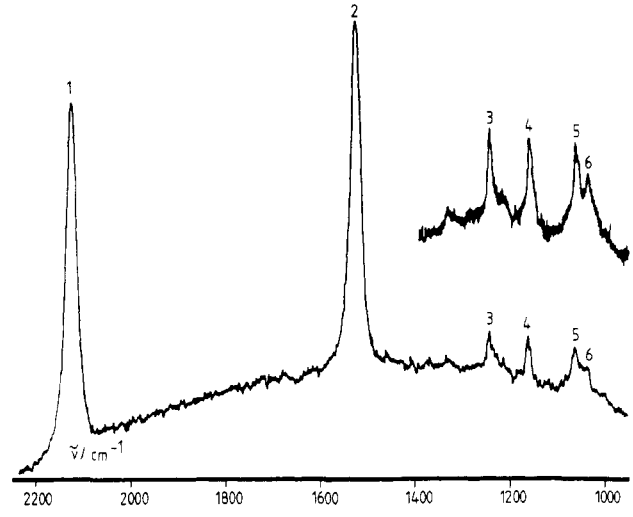

Figure 4. Raman spectrum of a solution of PTS-12 in chloroform (exciting wavelength at λ 648 nm).

In any case, these correlations between the Raman frequency and n_{eff} are based among others on the assumption that the molecule or rather the segment which is excited by the incident laser radiation is free from mechanical constraints such as stretching or bending forces, i.e., that the segment is fully coplanar and that bond lengths and angles do not deviate from their value determined by X-ray crystallography on the perfect crystals. On the other hand, it is well-known that the Raman bands of PDA crystals respond strongly to macroscopic strain exerted onto the crystals in the chain direction. Typically, a decrease in $\nu_{C=C}$ from 1498 to 1492 cm^{-1} is observed at a fractional elongation ($\Delta L/L$) of only 1%.[47,48] Unfortunately, the effect of bending or torsion has not been measured but a change of frequency by a similar magnitude has to be expected if the explanation given for the effect of stretching by Mitra et al.[47] is correct. These authors assumed that the decrease in multiple-bond frequencies observed experimentally with increasing tensile stress in the chain direction depends on force constant anharmonicities rather than on changes of the electronic structure of the backbone bonds.

(d) ^{13}C-NMR Spectra. The solution ^{13}C-NMR spectra of PTS-12 and of the corresponding monomer are shown

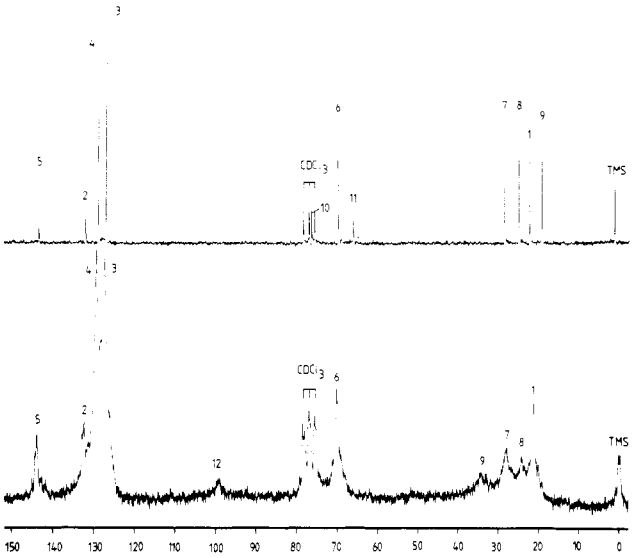

Figure 5. ^{13}C-NMR spectra of monomer (above) and polymer (below) PTS-12 (**4**) dissolved in $CDCl_3$.

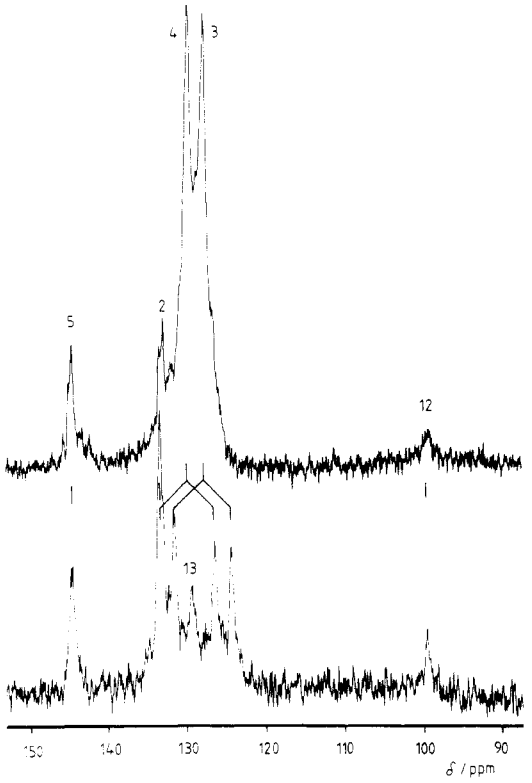

Figure 6. Section of the ^{13}C-NMR spectrum of PTS-12 with (above) and without (below) proton decoupling.

in Figure 5. The chemical shifts of the various signals and their identifications are summarized in Table IV. The signals were identified by comparison with literature data; the chemical shifts (δ-values) of some diacetylenes[49] and PDA[23,50] were determined some time ago.

The chemical shifts of the C atoms of the side chain remain essentially unaltered upon polymerization, with the exception of C-atom 12 adjacent to the triple bond in the monomer and to a double bond in the polymer. A downfield shift of $\Delta\delta$ = 16 is observed, in good correlation with the difference in the signal position of, e.g., the α-C atoms of 4-octyne and 4-octene ($\Delta\delta$ = 13).

The signal of the sp^2-hybridized backbone C-atom 13 is hidden under the signals of the C-atoms 3 and 4 of the tosylate side groups. It becomes observable, however, if

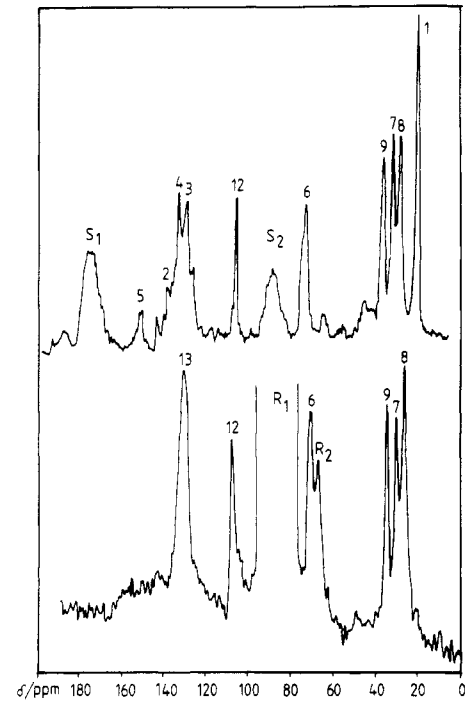

Figure 7. ^{13}C-NMR MAS spectra of crystalline PTS-12 (powder spectra) (for signal identification see Table IV): (top) normal polymer (**4**) (S_1 and S_2 are spinning side bands); (bottom) partially deuterated sample **13** (R_1 and R_2 are signals of the rotor material (POM "Hostaform").

the spectrum is recorded without proton decoupling, as demonstrated by Figure 6. The coupling of the C and H nuclear spins causes a splitting of the signals of all carbon atoms which are directly bound to a hydrogen (J_{CH} = 160 Hz). The signals of the quaternary C-atoms 2, 5, 12, and 13 remain unaltered, however.

The solid-state ^{13}C-NMR spectra are available by the magic angle spinning (MAS) technique. The ^{13}C-NMR MAS spectra of a polycrystalline (powder) sample of PTS-12 are shown in Figure 7. The chemical shifts observed are listed in Table IV; they are practically identical with those of the solution spectra as far as the side-group C atoms are concerned.

The signal of the sp^2-hybridized C-atom 13 is again hidden by the signals of the side-group C atoms. Problems with the signal-to-noise ratio prevent the use of the approach which we have taken in the case of the solution spectra to identify this signal. Another approach, namely, deuteration of the side groups, was highly successful. Replacement of the H atoms by D atoms increases the relaxation time of the excited ^{13}C spins. Additionally, the hyperfine interaction between the spin of the deuteron (S = 1) and that of the ^{13}C causes a splitting of each ^{13}C peak into a triplet. Both effects together cause a strong decrease in the signal intensity of all D-bound C atoms as compared to the quaternary ones. The ^{13}C-NMR MAS spectrum of partially deuterated PTS-12-d_{14} (**13**) is shown in Figure 7, with the signal of the backbone C-atom 13 now clearly visible.

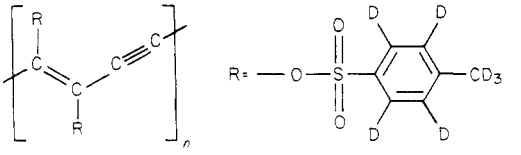

13

The signal of the sp-hybridized C-atom 12 suffers a

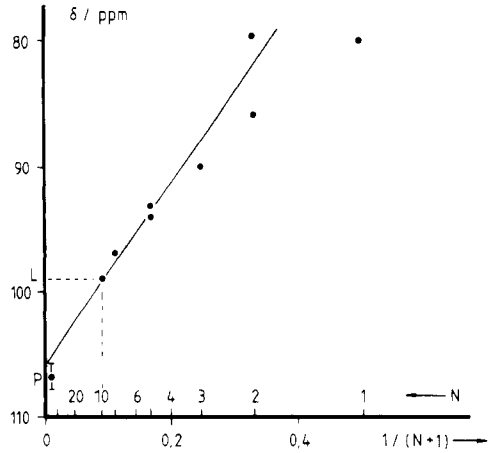

Figure 8. Chemical shifts of sp-hybridized C atoms in polyconjugated compounds as depending on the number of conjugated carbon bonds N: see also Table IV.

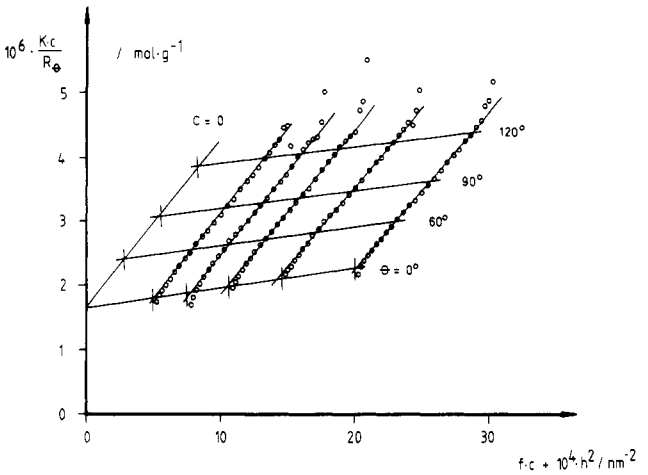

Figure 9. Zimm diagram of pristine PTS-12 (59% conversion) dissolved in 1,2-dichloroethane; λ 546 nm ($f = 1.65 \times 10^4$ cm^3 g^{-1}).

Table V
List of Model Compounds Illustrating the Effect of Conjugation on the Chemical Shift of an sp-Hybridized C Atom

no.	formula	N	δ	ref
14	$C_3H_7C=$	1	79.0	51
15	$-^aC=C^bCH_3$	2	85.7 (a), 79.8 (b)	52
16	$-C\equiv C-$	3	89.9	52
17	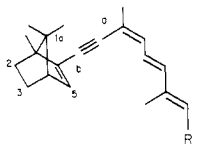	5	94.1 (a), 92.8 (b)	53
18	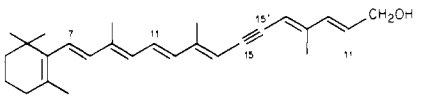	8	96.9	53
L	PTS-12, solution	10-12	99.4	this work
P	PTS-12, single crystal	>60	106-108	this work

downfield shift of $\Delta\delta = 9$ in going from the crystalline to the dissolved state, quite different from the sp^2-hybridized C atom, the position of which remains practically unaltered. A comparison with literature data reveals that the chemical shift of an sp-hybridized C atom depends to some extent on the number of multiple bonds to which it is conjugated. Figure 8 shows the chemical shift of a number of model compounds plotted vs. $1/(N+1)$, where N is the number of multiple bonds linked to the sp-hybridized C atom. These model compounds are listed in Table V; a phenyl ring in compounds **15** and **16** was counted as one double bond. The straight line which correlates the data in Figure 8 can be used as a calibration curve to determine the effective conjugation length of the dissolved PTS-12, especially since the data extrapolate reasonably well to the experimentally observed chemical shift of purely crystalline PTS-12 as the limiting case for very large N. The value of 99.4 ppm observed for dissolved PTS-12 corresponds to $12 < N < 10$, which translates into an n_{eff} of 5–6 constitutive units of the backbone, in excellent agreement with the results obtained by optical spectroscopy. Similarly, a value of 99.8 ppm was reported for the ^{13}C-NMR signal of the sp-hybridized C atom in the yellow solution of P3BCMU without any temperature dependence between 6 and 60 °C, and the polymers **7**, **8**, and **9** (Table I) dissolved in $CDCl_3$ show this signal at 99.5–99.7 ppm.[23]

The downfield shift of the ^{13}C-NMR signal with increasing conjugation length may be explained as being due to the small but increasing weight of a resonance admixture of a cumulene structure to the original enyne structure, as indicated below. The signal of a C atom in a pure cumulene structure is expected at $\delta = 200$.[54]

$$[=C-C\equiv C-C] \leftrightarrow [-C=C=C=C] \qquad (12)$$

In contrast to the sp-hybridized C atom, the sp^2-hybridized C atom does not change its electronic surroundings in going from resonance structure I to II as is obvious in looking at (12), and its ^{13}C-NMR signal does not therefore, depend on the conjugation length.

4. Solution Properties and the Molecular Shape of PDA

(a) Light Scattering Data on Pristine PTS-12 and P3BCMU. Light scattering measurements were performed on solutions of pristine PTS-12 and P3BCMU. The polymers were obtained by ^{60}Co γ-ray-induced polymerization in the solid state. Samples with 59% and 90% conversion to polymer were investigated in the case of PTS-12 and with 36% conversion in the case of P3BCMU. The UV–vis spectra of the solutions of these samples were identical with the ones shown in Figure 1, curve 2, and Figure 2, curve a.

The concentration and scattering angle dependent intensity of the light scattered from dilute solutions of these polymers was measured in a conventional light scattering photometer at λ 546 and 578 nm for PTS-12; in the case of P3BCMU, a laser light scattering photometer working at λ = 647.1 nm was used. The data analysis is described in the Experimental Section.

The Zimm diagram obtained for PTS-12 in 1,2-dichloroethane (59% conversion) is shown in Figure 9 and

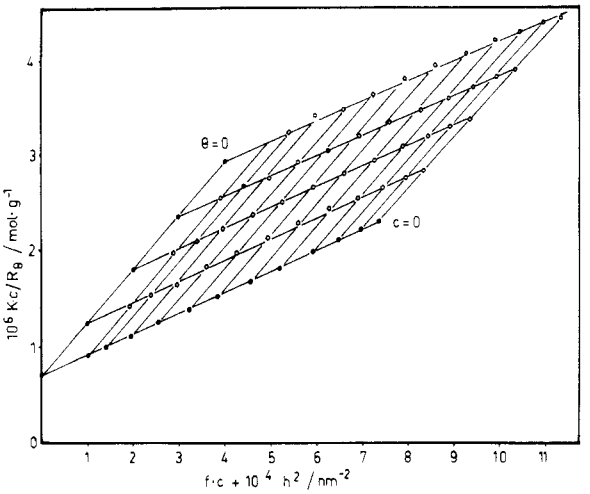

Figure 10. Zimm diagram of pristine P3BCMU (36% conversion) dissolved in $CHCl_3$; λ 647.6 nm.

Table VI
Results of the Light Scattering Investigation of Solutions of Pristine PTS-12[a] and P3BCMU[b]

polymer	conv %	λ/nm	$\bar{M}_w \times 10^{-3}$	$\langle S^2\rangle_z^{0.5}$/ nm	$10^4 A_2$/ (mol cm^3 g^{-2})
PTS-12	59	546	630	70.8	2.9
PTS-12	59	578	715	76.2	4.1
PTS-12	90	546	1430	118	2.0
P3BCMU	36	647	1360	94	5.4

[a] Dissolved in 1,2-dichloroethane. [b] Dissolved in $CHCl_3$.

the Zimm diagram for P3BCMU (36% percent conversion) dissolved in $CHCl_3$ is shown in Figure 10.

The usual evaluation of the Zimm diagram gives the data listed in Table VI. The linearity of the extrapolated function $Kc/R_\theta = f(c)$ and the positive values of the second virial coefficient in both cases show that the solvent used acts as a so-called good solvent for the polymer chain.

The angular dependence of Kc/R_θ gives some information about the shape of the macromolecule in solution.[55] To be independent from the size of the macromolecule, the reciprocal form factor $P_\theta^{-1} = M_w K_c/R_\theta$ is plotted vs. $u^2 = \langle S^2\rangle_z h^2$. As shown in Figure 11a for random coils a straight line with slope $^1/_3$ following eq 13 is obtained. A sample of monodisperse rodlike molecules exhibits a downward bent curve (Figure 11b) according to eq 14, in which t is an integration variable.[56] If one assumes in addition that the lengths of the rodlike molecules are distributed according to a normal (Schulz–Flory) distribution, a still more downward bent curve is expected,[57] as indicated by eq 15 and shown by Figure 11.

$$\frac{1}{P_\theta} = (Kc/R_\theta)M_w = 1 + {}^1/_3\langle S^2\rangle_z h^2 = 1 + {}^1/_3 u^2 \quad (13)$$

$$\frac{1}{P_\theta} = 3^{1/2}u\left[\int_{t=0}^{t=12^{1/2}u} \frac{\sin t}{t}\,dt - \frac{\sin (3^{1/2}u)}{3^{1/2}u}\right]^{-1} \quad (14)$$

$$\frac{1}{P_\theta} = u[\arctan u]^{-1} \quad (15)$$

It is obvious that the measured reciprocal form factors follow the straight-line behavior expected for coiled macromolecules and they deviate markedly from the curve c calculated for a polydisperse sample of rodlike polymer of the same contour length as assumed for the sample of randomly coiled molecules.

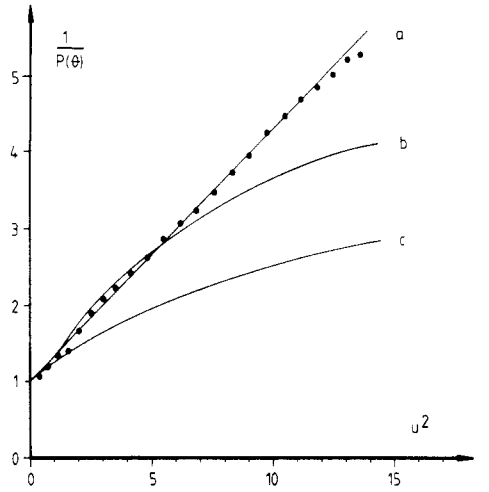

Figure 11. Plot of the reciprocal form factor P_θ^{-1} vs. $u^2 = h^2\langle S^2\rangle_z$ for PTS-12: (a) coils according to eq 11; (b) monodisperse rods according to eq 12; (c) rodlike molecules with normal distribution of lengths following eq 13. The solid points are experimental data from Figure 9.

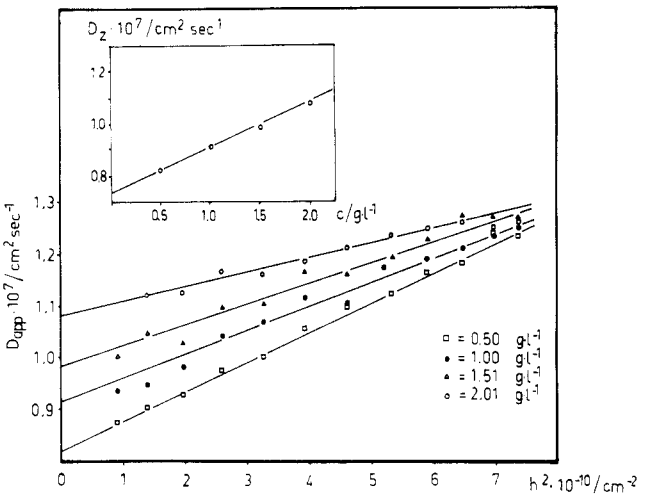

Figure 12. Dependence of the apparent diffusion constant of P3BCMU on the scattering vector h^2 and on concentration as measured by QLS.[31] $D_z = 0.725 \times 10^{-7}$ cm^2 s^{-1}, $R_H = 51$ nm, and $k_d = 240$ mL g^{-1}.

The assumption of a Schulz–Flory distribution of chain lengths is reasonable since the polymer sample investigated here was shown to have a polydispersity of M_w/M_n of approximately 2.[20]

The yellow solution of P3BCMU in $CHCl_3$ was further studied by quasi-elastic light scattering (QLS) in order to determine the hydrodynamic radius R_H, the translational diffusion constant D_z, and its concentration dependence expressed by the constant k_d (eq 8). A plot of the apparent diffusion constant D_{app} as depending on h^2 and the concentration dependence of D_z are shown in Figure 12. The experimentall determined radius of gyration of P3BCMU, 94 ± 2 nm, as well as the ratio of this magnitude to the hydrodynamic radius of $\langle S^2\rangle_z^{0.5}\langle 1/R_h\rangle_z = 1.85$ indicates a coillike shape of the molecules in solution; R_h is defined as an average by $R_H \equiv \langle 1/R_h\rangle_z^{-1}$.

The results of the integrated and of the quasi-elastic light scattering studies are summarized in Table VII and compared to the results of other authors on the same or other soluble PDAs. In light of the previous suggestion by Patel et al. that P3BCMU exists as a rodlike molecule in its yellow solution in DMF, the hypothetical radius of gyration was calculated according to eq 16 as if the samples

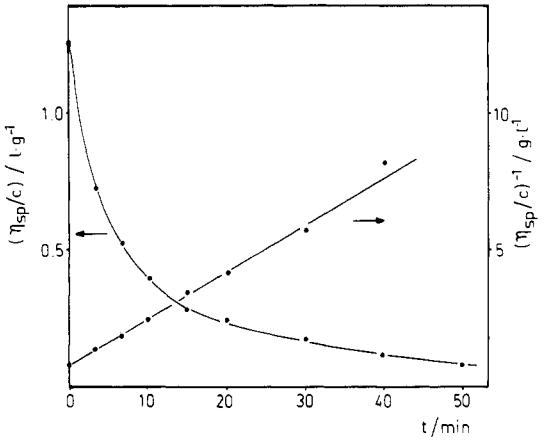

Figure 13. Photodegradation of P3BCMU dissolved in $CHCl_3$ in the course of irradiation by a Hg high-pressure lamp: (left) decrease of specific viscosity with time; (right) a plot according to eq 16.

consisted of monodisperse rods of molecular mass M_0 with a large ratio of length to cross section. The length l (0.49 nm) pertains to the constitutive unit of molar mass M_0; P is the degree of polymerization, which is given by $P = M/M_0$. The experimental value of M_w from ILS was used to approximate the numerical value of M.

$$\langle S^2\rangle^{0.5}_{rod} = (1/12^{1/2})lP \simeq (1/12^{1/2})L_w \qquad (16)$$

Since the samples are not monodisperse but exhibit a rather pronounced polydispersity, this has to be considered, making use of the theory of Goldstein.[20,57] Assuming a polydispersity of $M_w/M_n = 2$, the average square root radius of gyration expected is

$$\langle S^2\rangle^{0.5}_{SF\ rods} = 0.5L_w \qquad (17)$$

as was already pointed out in a preliminary publication[20] criticizing the conclusions drawn by Patel et al.[19]

One realizes on inspection of Table VII, where the calculated values of $(1/12^{1/2})L_w$ and $0.5L_w$ may be compared to the experimentally obtained $\langle S^2\rangle_z^{0.5}$ for different PDA polymers, that the experimental values are significantly smaller than the ones calculated from eq 16 or 17 and that they are well in the range expected for coiled, semiflexible molecules. It is interesting to note that this behavior is rather independent of the chemical nature of the particular substituent to the PDA backbone.

(b) Photodegradation of PDA and the Dependence of $\langle S^2\rangle_z$ on M_w. Further insights into the structure and properties of dissolved macromolecules are possible by investigating the depencence of the radius of gyration on the molecular weight. Samples of different molecular weights of PDA are readily obtained by photodegradation of solutions of the pristine polymers, which are usually of very high molecular weight (see Table VII). The photodegradation is understood as a random chain scission. It occurs rather independently of the nature of the side groups and is most probably a reaction involving free radicals; in other words, it can be enhanced by addition of photolabile radical initiators and it can be prevented by the addition of radical scavengers.[20,58] The occurrence of a random chain scission can be proven by measuring the decrease in specific viscosity (η_{sp}/c) with time under constant irradiation conditions. A simple relation holds in the case of random chain scission without depolymerization[59]

$$(\eta_{sp}/c)_t^{-1} = (\eta_{sp}/c)_{t=0}^{-1} + kt \qquad (18)$$

Here, t is the time of irradiation, k is a rate constant, and the indices relate to the specific viscosity at the time t_0 at the beginning and at the actual time t.

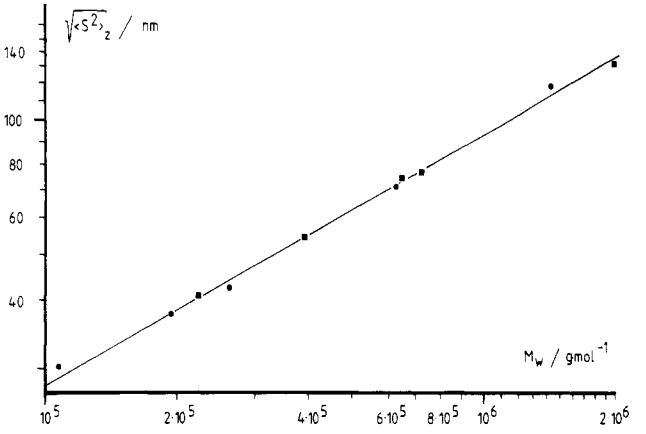

Figure 14. Dependence of $\langle S^2\rangle_z$ on M_w for PTS-12 dissolved in 1,2-dichloroethane; data points obtained by ILS at λ 546 nm (○) and λ 578 nm (■), each point representing a different sample.

A plot showing this relationship for the special case of P3BCMU is presented in Figure 13; the same behavior has been found for many different PDA.[60] The fact that a random chain scission without depolymerization always produces a normal distribution of chain length is also very helpful for our purpose. There are no other reactions besides the chain degradation.

This photodegradation behavior of PDA was used to prepare a series of samples of PTS-12 starting from a solution of the high molecular weight pristine polymer. These samples were then investigated by ILS, and the dependence of $\langle S^2\rangle_z$ on M_w was derived. The data are shown in Figure 14 and may be represented by

$$\langle S^2\rangle_z^{0.5} = 0.45M_w^{0.55} \qquad (19)$$

Note that the data of the pristine and of the photodegraded polymer fall on the same line and that the relationship given by eq 19 holds over a wide range of M_w.

A sample consisting of random coils under Θ-conditions is expected to show an exponent with regard to M_w of 0.5 (neglecting excluded volume effects in the present discussion); if the sample consisted of rodlike molecules, an exponent of 1 should be found. Coiled macromolecules in good solvents show exponents between 0.55 and 0.65.[55]

Furthermore, the viscosity behavior is in full agreement with the above findings and completely within the expectations for a sample consisting of random coiled macromolecules. The specific viscosity is found to depend linearly on concentration following the Huggins equation

$$(\eta_{sp/c}) = [\eta] + [\eta]^2K_Hc \qquad (20)$$

where $[\eta]$ (mL g^{-1}) is the Staudinger index and K_H is the Huggins constant. Typically, a sample of PTS-12 of $M_w = 143 \times 10^4$ g dissolved in $CHCl_3$ showed $K_H = 0.45$, indicating that $CHCl_3$ acts as a good solvent for the polymer.

Finally, the relationship between the limiting viscosity number $[\eta]$ (Staudinger index) and the molecular weight can be investigated. The $[\eta]$–M_w relationship for PTS-12 in $CHCl_3$ (25 °C) is shown in Figure 15. It is described by

$$[\eta] = 6.4 \times 10^{-3}M_w^{0.83} \qquad (21)$$

The value of the exponent to M_w in eq 21 allows one to conclude the shape of the molecules as well. A value of 0.5 should be found for random coils under Θ-conditions, and the exponent should be 2 for rodlike molecules. The actual value is indicative of coiled macromolecules under conditions of a good solvent.

Table VII
Comparison of the Results of Light Scattering Studies on Solutions of Various PDAs of General Structure 1

polymer[a]	ref	solvent	$10^{-4}M_w$	$\bar{P}_w$	M_w/M_n	$(1/2)L_w$/ nm	$(1/12^{1/2})L_w$/ nm	$\langle S^2\rangle_z^{0.5}$/ nm	$A_2 \times 10^4$/ (mol cm^3 g^{-2})
PTS-12	this work; cf. Figure 9	CH_2ClCH_2Cl	63	1253	2.66	307	177	70.8	2.9
P3BCMU[b]	this work; cf. Figure 10	$CHCl_3$	136	2830		693	400	94 ± 2	5.4
P3BCMU	19	DMF	49	1020	5.0	250	144	150 ± 50	
7	23	$CHCl_3$	80	1700	3.33	416	240	110	7.0
8	23	$CHCl_3$	134	2300	3.94	563	325	131	6.9
9	23	$CHCl_3$	120	1800	3.75	441	254	126	5.2

[a] See Table I for abbreviations. [b] This sample showed $D_z = 0.725 \times 10^{-7}$ cm^2 s^{-1}, $R_H = 51$ nm, and $k_d = 240$ mL g^{-1} by QLS; see Figure 12.

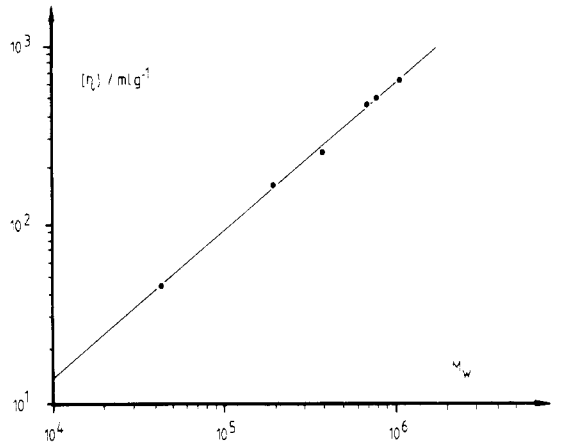

Figure 15. $[\eta]$–M_w relationship for PTS-12 in $CHCl_3$ at 25 °C.

(c) PTS-12: An Example of a Wormlike Chain. The data collected so far on the solution behavior of PDA chains can be readily discussed in terms of the wormlike chain (Porod–Kratky chain).[61,62] This concept for a chain molecule visualizes a continuous curvature of the chain skeleton, the direction of curvature at any point of the trajectory being random. In terms of this concept the stiffness of the chain is characterized by the average value of the projection of the $i + 1$ segment of the chain into the direction of the ith segment denoted by $\langle \cos \alpha \rangle$,$\alpha$ being the angle between the directions of the two consecutive segments. The so-called persistence length l_{pers} is then defined by

$$l_{pers} = 1/(1 - \langle \cos \alpha \rangle) \tag{22}$$

The radius of gyration of the wormlike chain is then calculated from the persistence length and the contour length $L = Pl$ by eq 23, where $y = L/l_{pers}$ is called the reduced

$$\langle S^2 \rangle = \frac{2L^2}{y^4}(-1 + y - \tfrac{1}{2}y^2 + \tfrac{1}{6}y^3 + e^{-y}) \tag{23}$$

contour length. Values calculated according to eq 23 cannot be compared to our experimental data since the polydispersity of the actual sample is not yet considered. This can be done by calculating the z average of $\langle S^2 \rangle$ of an ensemble of wormlike chains with a Schulz–Flory distribution ($M_w/M_n = 2$) of the contour lengths according to

$$\langle S^2 \rangle_z = \frac{\sum_P \langle S^2 \rangle P^3 (1 - 2/P_w)^P}{\sum_P P^3 (1 - 2/P_w)^P} \tag{24}$$

The characteristic ratio C_p may now be calculated. It is given by

$$C_p = 6\langle S^2 \rangle_z / P_w l^2 \tag{25}$$

and plotted as a function of P_w in Figure 16, where l_{pers} is used as the prefixed parameter. The characteristic ratio of the wormlike chain increases initially with increasing degree of polymerization but it will soon reach a plateau value. The limiting value of C_p increases with an increase of persistence length. The curves in Figure 16 are interpreted such that the initial linear increase of C_p with the chain length models the behavior of a stiff rod, and the constant value in the plateau region describes that of a random coil. The overall graph describes, therefore, that even very stiff chains assume the properties of a random coil, if their length is only large enough.

Table VIII
Persistence Length of Some Polymers with Large Stiffness

polymer	M_w/M_n	solvent	M_L/(g mol^{-1} nm^{-1})	d/nm	$l_{pers}^{(L)}$[a]/ nm	$l_{pers}^{(V)}$[b]/ nm	ref
PTS-12	2.6	1,2-dichloroethane	1060	1.1	19.0	15.0[c]	this work
cellulose nitrate	1.1	acetone	520	0.4	20.0	16.5	63, 65
poly(hexyl isocyanate)	1.1	hexane	710	1.64	41.0	41.0	66
DNA		aqueous NaCl	1950	2.5	57.5	56.5	63, 67

[a] Derived from ILS. [b] By viscosity measurements. [c] Determined for $CHCl_3$ as solvent.

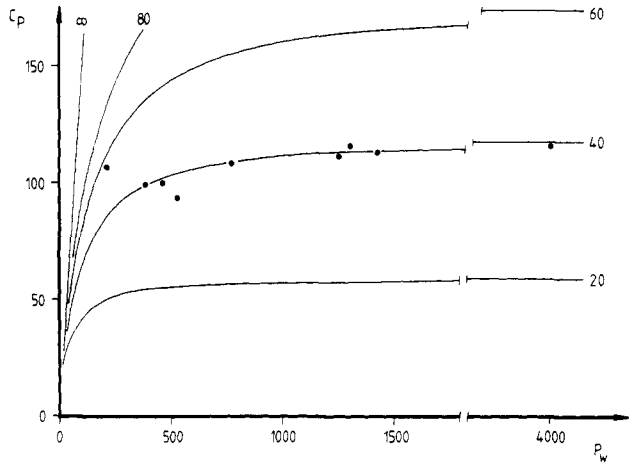

Figure 16. Characteristic ratio C_p vs. degree of polymerization P_w: solid lines, calculated for a wormlike chain with the persistence length l_{pers} (in number of monomer units) as the parameter; points, results from ILS (data from Figure 14).

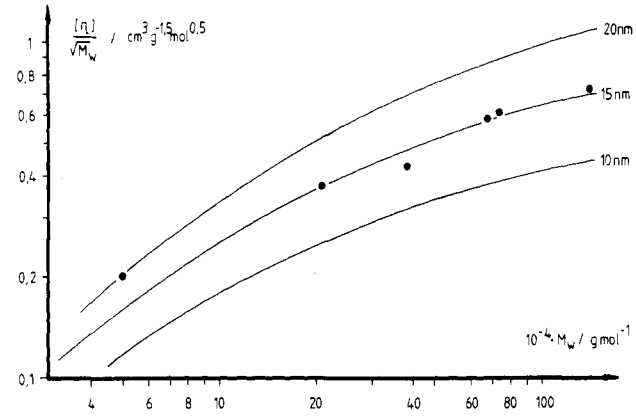

Figure 17. $[\eta]/M^{1/2}$ vs. the molecular mass M_w of a wormlike chain. The parameter given at the curves is the persistence length l_{pers} in nm. The solid points are experimental data taken from Figure 15.

The data reported in Figure 14 can be used to derive the experimental value of C_p depending on P_w. These data are included in Figure 16. It is realized that the curve describing the behavior of a wormlike chain with a persistence length of 40 monomer units (~19.0 nm) fits the experimental data very well.

Yamakawa and Fujii[63] have shown how the Staudinger index of a wormlike chain can be calculated

$$\frac{[\eta]}{M^{1/2}} = \phi\left(\frac{2l_{pers}}{M_L}\right)^{3/2} \qquad (26)$$

$M_L = M_0/l$ is the molar mass per unit length and ϕ is a magnitude depending in its numerical value on the reduced thickness $d_r = d/2l_{pers}$ and the reduced contour length $L_r = L/2l_{pers}$ of the polymer chain. The limiting value of ϕ for $L_r \to \infty$ and $d_r \to 0$ is Flory's constant[64] $\phi^\infty = 2.84 \times 10^{23}$ mol^{-1}. The numerical values of ϕ have been tabulated by the above-mentioned authors.[63]

The thickness of the PTS-12 chain was approximated to be 1.0 nm in accordance with the known cross section per chain in the perfect single crystals of the polymer.[32] The final result is not very sensitive to the exact value of ϕ so that this approximation, which neglects conformational changes in the side groups due to solvent interactions, seemed to be sufficient.

A polydispersity correction of eq 26 is not necessary since the weight- and the viscosity-average molecular weights are practically identical in the present case due to the special value of the exponent of M in the experimental $[\eta]$–M_w correlation (eq 21).

The ratio $[\eta]/M^{1/2}$ is plotted vs. M in Figure 17, the persistence length being again the parameter. The solid points are experimental data taken from Figure 15. They fit the curve calculated for a wormlike chain of l_{pers} = 15.0 nm (31 monomer units) reasonably well. The agreement between the viscosimetrically determined and ILS-derived persistence length is reasonably good within the limits of the approximations made in the calculations. It is also worth mentioning that excluded volume effects have not been considered, which would help to further optimize the agreement between the two methods.

Since we only like to point out the wormlike nature of the PDA chain using PTS-12 as an example, we leave a further detailed discussion of this and other effects to further work. We like, however, to compare the results on the chain stiffness to what is known on other stiff polymers. For this purpose data on some other polymers known to behave as wormlike chains do are collected in Table VIII. Most polymers which have a larger persistence length than PTS-12 form a helixlike superstructure in solution, and it is the interaction between the side groups of the polymer backbone which stabilizes the helix and induces the chain stiffness. Contrary to that, the stiffness of the PDA chain is only caused by the polyconjugated structure of the backbone and is rather independent of the nature of the side groups (see, e.g., Table VII).

To get a better feeling for the curvature of the PDA chain in solution, we can calculate the average of the angle α used for the definition of the persistence length in eq 22. An angle of $\alpha = 12.6°$ per constitutive unit is derived by using 19.0 nm as the persistence length of PTS-12. If we now assume for the purpose of an approximation that all four carbon bonds within the constitutive unit are bent by the same amount, an average deformation of 3.2° per bond is necessary to produce the experimentally observed behavior.

A final remark to this section is concerned with the structural purity of the PDA chain. One could argue that the introduction of a few cis double bonds into the otherwise pure *trans*-PDA chain would be sufficient to produce enough segmental mobility to cause the behavior of a coil in solution. We were, however, unable to detect any sign for the presence of cis double bonds (or any other "impurity" structure) by spectroscopic means (see the section on Raman and ^{13}C spectroscopy), and all experi-

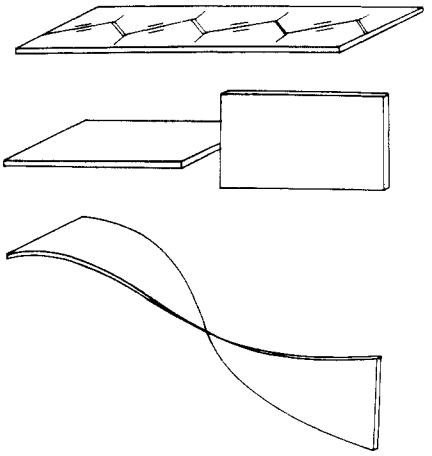

Figure 18. Shape of the PDA chain: (a) planar structure in the crystal; (b) two segments in solution in terms of the Kuhn chain (note that adjacent segments are electronically decoupled due to bond rotation and that the bond connecting two segments has the character of a local defect); (c) part of wormlike chain with continuous curvature of the chain skeleton.

ments to produce the cis structure deliberately by photoinduced or catalytic cis–trans isomerization led to the straightforward random chain scission described above rather than to the intended cis structure. We are, therefore, left with the conclusion that we have described the behavior of a structurally pure polyconjugated macromolecule.

Within the concept of the wormlike chain, the continuous curvature of the chain skeleton does not have a limit as we approach smaller and smaller segments and finally reach a segment of the length of the constitutive unit. This is indicated by Figure 18, where the shape of the wormlike chain is compared to the shape of a random flight chain (Kuhn chain) over distances which do not comprise more than approximately 10 conjugated bonds of the backbone. It is now fairly obvious that the discussion of a so-called effective conjugation length (see section 3) is rather difficult to translate into the concept of the wormlike chain, although its meaning is perfectly clear in terms of the Kuhn model. To the best of our knowledge, the effect of a continuous curvature on the electronic behavior of a polyconjugated sytem has not been investigated experimentally nor theoretically so far and the data presented here may thus very well be the first ones in which the effects of such a curvature have been noted.

5. Yellow-to-Blue Transition of P3BCMU

(a) Kinetics of the Transition. P3BCMU and other PDAs with similar side groups have been noted to undergo dramatic color changes when the solvent to nonsolvent ratio or the temperature in certain solvent/nonsolvent mixtures is changed.[18] A model has been proposed which assigns the color change to a "visual" nonplanar–planar conformational transition involving a dramatic alteration of the average conjugation length from 4–7 repeat units in the yellow to essentially infinite in the blue "solution".[18,25,36] The effect has already been demonstrated by Figure 2.

Since we have shown in the previous section that the concept of effective conjugation length used by the above-cited authors is open to a discussion, we now investigate the assumed "conformational transition" somewhat more closely.

A sample of P3BCMU (M_w = 1.36 × 10^6) was dissolved in chloroform in which P3BCMU forms a yellow solution at practically any concentration. Addition of *n*-hexane to

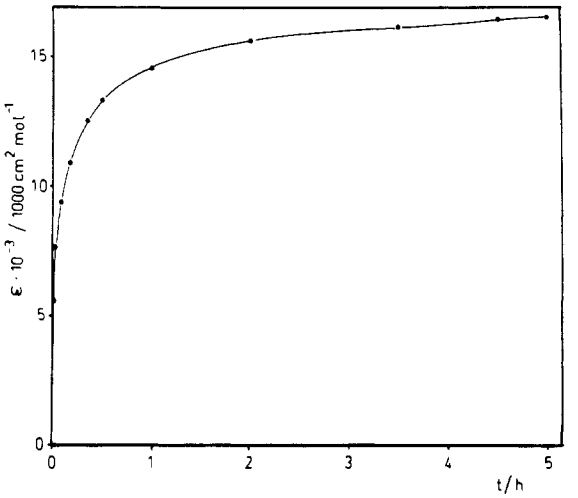

Figure 19. Growth of the 630-nm peak ("blue" form) with time (T = 25 °C) after addition of *n*-hexane to the "yellow" solution of P3BCMU (M_w = 1.36 × 10^6) in chloroform so as to obtain a ratio of 65:35 (v/v) of the solution (c_{P3BCMU} was 0.034 and 0.017 g L^{-1}).

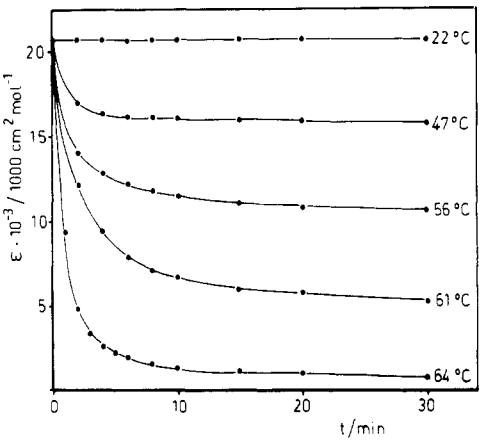

Figure 20. Transition from the blue to the yellow form of P3BCMU (M_w = 1.36 × 10^6) upon heating a solution in 1,2-dichloroethane (c = 0.0178 g L^{-1}) from 22 °C to the temperatures indicated. The apparent extinction at 630 nm is plotted vs. time. The temperature adjustment was reached at t < 2 min.

the yellow solution causes the immediate precipitation of P3BCMU in the blue form if the concentration is larger than 0.4 g L^{-1} at room temperature. Solutions with c < 0.4 g L^{-1} show the color change noted by Figure 2 and seem to give a stable blue state if the $CHCl_3$/*n*-hexane ratio is adjusted to 65:35 (v/v) at room temperature.

The color change is reversible with temperature. Heating of the blue polymer solution at room temperature in, e.g., 1,2-dichloroethane to 70 °C causes the transformation to yellow; the blue form is regained upon cooling to room temperature.

This visual transition is seen to show rather peculiar kinetics if followed spectrophotometrically. It turns out that it is difficult to reach an equilibrium blue state and that the relative concentration of the blue vs. the yellow form in a given solvent system is dependent not only on time and temperature but also on the history of the sample, as is commonly observed in nucleation-controlled crystallization or aggregation phenomena. The effects are demonstrated by Figures 19–21. Figure 19 shows the time dependence of the extinction at 630 nm (peak maximum of the "blue" form) of a solution of the polymer, which was initially prepared in chloroform and to which *n*-hexane had been added so as to instantaneously adjust the solvent ratio

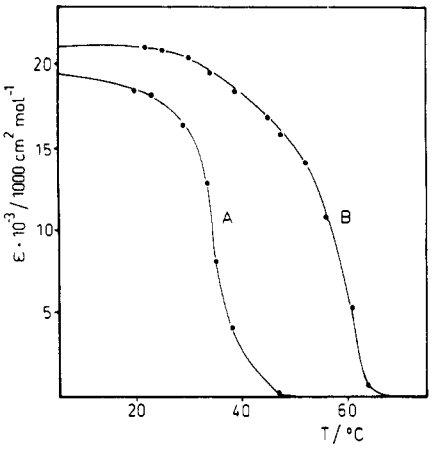

Figure 21. Hysteresis of the blue-to-yellow transition of P3BCMU in 1,2-dichloroethane as characterized by the apparent extinction ϵ at 630 nm reached after 20 min when a solution of c_{P3BCMU} = 0.0178 g L^{-1} was cooled from 70 °C to the temperature indicated on the abscissa (curve A) and when it was heated to the temperature indicated on the abscissa (curve B).

to the above-mentioned ratio of 65:35. The blue peak grows logarithmically and the final value around 20×10^3 (1000 cm^2 mol^{-1}) is only reached after about 2 days, after which time sometimes the formation of a blue precipitate is observed.

The reverse of the process is shown in Figure 20. Here, the blue "solution" of P3BCMU was instantaneously heated to the temperature indicated, and the disappearance of 630-nm absorption was monitored with time. Different equilibrium values are reached at different temperatures as indicated by Figure 20. The final value reached depends, however, on whether it has been approached starting from the high-temperature (yellow) or the low-temperature (blue) form (Figure 21). In other words, pronounced hysteresis is seen, which makes it difficult to perform any measurement on the pure "blue" form or to investigate the thermodynamics of this interesting phenomenon.

(b) Changes in the State of Aggregation in Going from the Yellow to the Blue Form. The yellow solution of P3BCMU is formed by molecularly dispersed macromolecules as indicated by the ILS data (see Figure 10). This is not the case for the blue solutions. This was first recognized when we tried to purify the so-called blue solutions for light scattering measurements. Contrary to the yellow solutions (M_w = 1.36 × 10^6) which can be filtered through 0.5-μm millipore filters without any loss, the polymer is completely removed by filtering a blue solution through a Millipore filter of 1.2-μm width of the pores. Even when we used filters of 3-μm width of the pores, more than 20% of the polymer was removed after filtration, as was readily monitored by measuring the decrease in concentration spectrophotometrically. This is true for the blue solutions in 1,2-dichloroethane as well as in $CHCl_3$/*n*-hexane.

Next we tried to measure the light scattering intensity of the blue solution which had been purified in the yellow form and which we had conditioned at room temperature for 60 h so as to reach an apparent equilibrium value of transformation which would not further change in the time necessary for ILS measurements. A dramatic increase in light scattering intensity was noted as compared to the yellow solutions at the same concentration and wavelength. The overall concentration of the polymer had thus to be reduced to values of $c < 0.01$ g L^{-1} as compared to the yellow solutions, where reasonable measurements could only be made at $c > 0.5$ g L^{-1}. Although we were unable to determine the refractive index increment for the blue polymer form due to the fact that at reasonable concentrations for the measurement the polymer precipitates in the form of blue flakes, we nevertheless describe the scattering effects.

Table IX
Comparison of the Intensity of the Scattered Light by a "Yellow" and a "Blue" Solution[a] of P3BCMU of Equal Concentration (c = 0.0096 g L^{-1}) at θ = 90°

state of P3BCMU solution	λ/nm	$I_\theta(90°)$[b]/ au	R_θ/cm^{-1}
blue	436	19.4	1.21 × 10^{-4}
yellow	436	1.2	~0
blue	546	63.3	6.71 × 10^{-4}
yellow	546	8.4	~0
blue	578	40.0	9.89 × 10^{-4}
yellow	578	4.0	~0

[a] Blue solution in 1,2-dichloroethane; yellow solution in chloroform; M_w of the polymer in the yellow solution 1.36 × 10^6; see Zimm diagram in Figure 10. [b] Corrected for absorption (see Experimental Section).

The data obtained by ILS of the sample of P3BCMU of which the Zimm diagram is shown in Figure 10 are summarized in Table IX.

It is readily seen that the so-called blue solution shows a tremendous intensity of the scattered light as compared to the yellow solution. In a very crude approximation one can use the refractive index increment of the yellow solution determined at 578 nm in $CHCl_3$ in order to convert the measured scattering intensity at 578 nm to an approximate molecular weight. An approximate $M_w = 2 \times 10^8$ is then calculated (compared to M_w = 1.36 × 10^6 for the yellow form); the blue form must then be an aggregation of at least 150 chains in what we think is a microcrystal or semicrystalline gel particle.[68]

Further work by QLS is in progress to better characterize the hydrodynamic properties of these particles.

Although these results do not explain the origin of the yellow-to-blue color shift, they rule out, at least, that we are dealing with a pure intramolecular effect. Note that the spectrum of the so-called blue solutions is very similar to the spectrum of the pristine single crystal and to the spectrum of the recrystallized polymer. One is thus tempted to argue that the blue spectrum is characteristic of the P3BCMU chain in a crystalline surrounding and that the origin of the blue color, i.e., the red shift of the absorption, is due to intermolecular interactions of the chains either in the ground state or, more probably, in their photoexcited state.

6. Conclusions

PDA chains as models of soluble polyconjugated macromolecules behave like wormlike chains in solutions. These solutions are characterized by a bright yellow to orange color (λ_{max} ~460 nm). Resonance-Raman and ^{13}C-NMR data as well as the energy of the optical transition can be interpreted as if the dissolved chain molecules exhibit a so-called effective conjugation length as compared to the single-crystal state in which a fully extended coplanar structure of the backbone is found. The characterization of the chain as wormlike (see Figure 18) implies, however, a continuous deformation of the backbone skeleton down to the scale of the constitutive unit of the macromolecule. The model of a continuously deformed polyconjugated backbone is thus developed as opposed to a local defect model in which the effective conjugation length is caused by bond rotation which removes the coplanarity of adjacent segments of the chain but leaves the

backbone atoms within the segment coplanar. The chain stiffness of PTS-12 has been determined and characterized by the persistence length l_{pers} = 15–19 nm (30–40 constitutive units) as compared to the value of the effective conjugation length n_{eff} = 6–7 constitutive units.

The visual yellow-to-blue transition occurring in solutions of P3BCMU if the temperature or solvent quality is changed has been kinetically characterized and preliminary data on ILS are presented. The effect is described as an aggregation phenomenon. In the blue state a microgel or semicrystalline colloidal particle is formed consisting of ca. 150 individual chains under the conditions investigated. Earlier models of other authors[15,18,36] implying that the yellow-to-blue transition is purely intramolecular are thus ruled out.

Acknowledgment. This work was supported by a grant from the Stiftung Volkswagenwerk. Further financial support by the Fonds der Chemischen Industrie is acknowledged. We also thank Dr. V. Enkelmann and Dr. C. Bubeck for helpful discussions and suggestions.

Registry No. 3, 68810-64-0; 4, 89105-99-7; PTS-12, 89163-41-7; P3BCMU, 89163-42-8.

References and Notes

(1) Wegner, G. *Z. Naturforsch., B* **1969**, *24B*, 824.
(2) Wegner, G. *Makromol. Chem.* **1971**, *145*, 85.
(3) Wegner, G. In "Molecular Metals"; Hatfield, W. E., Ed.; Plenum Press: New York, 1979; p 209f.
(4) Baughman, R. H. *J. Appl. Phys.* **1972**, *43*, 4362.
(5) Baughman, R. H. *J. Polym. Sci., Polym. Phys. Ed.* **1974**, *12*, 1511.
(6) Bloor, D. In "Developments in Crystalline Polymers"; Basset, D. C., Ed.; Applied Science Publishers: London, 1982; p 155f.
(7) Bloor, D.; Preston, F. H.; Ando, D. J.; Batchelder, D. N. In "Structural Studies of Macromolecules by Spectroscopic Methods"; Ivin, K. J., Ed.; Wiley: New York, 1976; p 91f.
(8) Enkelmann, V. Habilitationsschrift, University of Freiburg, FRG.
(9) Enkelmann, V.; Leyrer, R. J.; Wegner, G. *Makromol. Chem.* **1979**, *180*, 1787.
(10) Enkelmann, V.; Leyrer, R. J.; Schleier, G.; Wegner, G. *J. Mater. Sci.* **1980**, *15*, 168.
(11) Bubeck, C.; Sixl, H.; Neumann, W. *Chem. Phys.* **1980**, *48*, 269.
(12) Hartl, W.; Schwoerer, M. *Chem. Phys.* **1982**, *69*, 443.
(13) Niederwald, H.; Eichele, H.; Schwoerer, M. *Chem. Phys. Lett.* **1980**, *72*, 242.
(14) Eckhardt, H.; Prusik, T.; Chance, R. R. *Macromolecules* **1983**, *16*, 732.
(15) Baughman, R. H.; Chance, R. R. *Ann. N.Y. Acad. Sci. Sci.* **1978**, *313*, 705.
(16) (a) Wegner, G. *Pure Appl. Chem.* **1977**, *49*, 443. (b) Wegner, G. *J. Polym. Sci., Polym. Lett. Ed.* **1971**, *9*, 133.
(17) Patel, G. N. *J. Polym. Sci., Polym. Lett. Ed.* **1978**, *16*, 607.
(18) Patel, G. N.; Chance, R. R.; Witt, J. D. *J. Chem. Phys.* **1979**, *70*, 4387.
(19) Patel, G. N.; Walsh, E. K.*J. Polym. Sci., Polym Lett. Ed.* **1979**, *17*, 203.
(20) Wenz, G.; Wegner, G. *Makromol. Chem. Rapid Commun.* **1982**, *3*, 231.
(21) Tieke, B.; Graf, H.-J.; Wegner, G.; Naegele, B.; Ringsdorf, H.; Banerjie, H.; Day, D.; Lando, J. B. *Colloid Polym. Sci.* **1977**, *255*, 521.
(22) Plachetta, C.; Rau, N. O.; Hauck, A.; Schulz, R. C. *Makromol. Chem., Rapid Commun.* **1982**, *3*, 249.
(23) Plachetta, C.; Schulz, R. C. *Makromol. Chem., Rapid Commun.* **1982**, *3*, 815.
(24) Arndt, G. Ph.D. Thesis, University Mainz, Mainz, FRG, 1975.
(25) Chance, R. R.; Shand, M. L.; Le Postollec, M.; Schott, M. *J. Polym. Sci., Polym. Lett. Ed.* **1981**, *19*, 529.
(26) Note, however, the recent reports on soluble block copolymers of acetylene: Bates, F. S.; Baker, G. L. *Macromolecules* **1983**, *16*, 1013.
(27) Kuzmany, H. *Phys. Status Solidi B* **1980**, *97*, 521.
(28) Piseri, L.; Tubino, R.; Paltrinieri, L.; Dellepiane, G. *Solid State Commun.* **1983**, *46*, 183.
(29) Kuzmany, H.; Imhoff, E. A.; Fitchen, D. B.; Sarhangi, A. *Phys. Rev. B* **1982**, *26*, 7109.
(30) Patel, G. N. *Polym. Prepr., Am. Chem. Soc., Div. Polym. Chem.* **1978**, *19*, 154.
(31) Bantle, S.; Schmidt, M.; Burchard, W. *Macromolecules* **1982**, *15*, 1604.
(32) Siegel, D.; Sixl, H.; Enkelmann, V.; Wenz, G. *Chem. Phys.* **1982**, *72*, 201.
(33) Wenz, G. Ph.D. Thesis University of Freiburg, FRG.
(34) Exarhos, G. J.; Risen, W. H.; Baughman, R. H. *J. Am. Chem. Soc.* **1976**, *98*, 481.
(35) Baughman, R. H.; Chance, R. R. *J. Polym. Sci., Polym. Phys. Ed.* **1976**, *14*, 2037.
(36) Chance, R. R. *Macromolecules* **1980**, *13*, 396.
(37) Kuhn, H. *Fortschr. Chem. Org. Naturst.* **1958**, *16*, 169; **1959**, *17*, 404.
(38) Bohlmann, F. *Ber. Dtsch. Chem. Ges.* **1953**, *86*, 657.
(39) Bohlmann, F.; Mannhardt, H. J. *Ber. Dtsch. Chem. Ges.* **1956**, *89*, 1307.
(40) Rimai, L.; Heyde, M. E.; Gill, D. *J. Am. Chem. Soc.* **1973**, *95*, 4493.
(41) Bohlmann, F.; Polit, K. *Ber. Dtsch. Chem. Ges.* **1957**, *90*, 130.
(42) Bloor, D.; Batchelder, D. N.; Ando, D. J.; Read, R. T.; Young, R. J. *J. Polym. Sci., Polym. Phys. Ed.* **1981**, *19*, 321.
(43) Naylor, P.; Whiting, M. C. *J. Chem. Soc.* **1955**, 3042.
(44) Baughman, R. J.; Witt, J. D.; Yee, K. C. *J. Chem. Phys.* **1974**, *60*, 4755.
(45) Shand, H. L.; Chance, R. R.; Le Postollec, M.; Schott, M. *Phys. Rev. B* **1982**, *25*, 4431.
(46) Ivanova, T. M.; Yanovskaya, L. A.; Shorygin, P. P. *Opt. Spectrosc.* **1965**, *18*, 115.
(47) Mitra, V. K.; Risen, W. M., Jr.; Baughman, R. H. *J. Chem. Phys.* **1977**, *66*, 2731.
(48) Lewis, W. F.; Batchelder, D. N. *Chem. Phys. Lett.* **1979**, *60*, 232.
(49) Traficante, D. D.; Maciel, G. E. *J. Phys. Chem.* **1965**, *69*, 1348.
(50) Babitt, G. E. Patel, G. N. *Macromolecules* **1981**, *14*, 554.
(51) Breitmaier, E.; Voelter, W. "^{13}C-NMR-Spectroscopy", 2nd ed.; Verlag Chemie: Weinheim, FRG, 1978.
(52) Levy, G. C.; Nelson, G. L. "Carbon-13 Nuclear Magnetic Resonance for Organic Chemists"; Wiley: New York, 1972.
(53) Englert, G. *Helv. Chim. Acta* **1975**, *58*, 2367.
(54) Crandall, J. H.; Sojka, S. A. *J. Am. Chem. Soc.* **1972**, *94*, 5084.
(55) Burchard, W. In "Applied Fibre Science"; Happey, F., Ed.; Academic Press: New York, 1978; Vol. 1, Chapter 10, p 381f.
(56) Neugebauer, T. *Ann. Phys.* **1943**, *42*, 509.
(57) Goldstein, H. *J. Chem. Phys.* **1953**, *21*, 1255.
(58) Müller, M. A.; Wegner, G. *Makromol. Chem., Rapid Commun.*, in press.
(59) (a) Delzenne, G.; Smets, G. *Makromol. Chem.* **1955**, *18*, 82. (b) Ranby, B.; Rabek, J. F. "Photodegradation, Photooxidation and Photostabilization of Polymers"; Wiley: New York, 1975; p 76f.
(60) Müller, M. A.; Wegner, G., unpublished results.
(61) (a) Porod, G. *Monatsh. Chem.* **1949**, *80*, 251. (b) Kratky, O.; Prod, G. *Recl. Trav. Chim. Pays-Bas* **1949**, *68*, 1106.
(62) Flory, P. J. "Statistical Mechanics of Chain Molecules"; Interscience: New York, 1969; p 401f.
(63) Yamakawa, H.; Fujii, H. *Macromolecules* **1974**, *7*, 128.
(64) Reference 62, p 35f.
(65) Meyerhoff, G. *J. Polym. Sci.* **1958**, *29*, 399.
(66) Rubingh, D. N.; Yu, M. *Macromolecules* **1976**, *9*, 681.
(67) Kirste, R. G. *Discuss. Faraday Soc.* **1970**, *49*, 81.
(68) The possibility that the large intensity of the scattered light observed from the blue form of P3BCMU is to a large part due to a resonance enhancement of the Raleigh process can be ruled out as will be discussed elsewhere (Müller, M. A.; Schmidt, M.; Wegner, G. *Makromol. Chem., Rapid Commun.* **1984**, *5*, 83.